



New orange–red phosphor $\text{Sr}_9\text{Sc}(\text{PO}_4)_7:\text{Eu}^{3+}$ for NUV-LEDs application



Xiaoling Dong^{a,b}, Jiahua Zhang^{a,*}, Xia Zhang^a, Zhendong Hao^a, Yongshi Luo^a

^a Key Laboratory of Luminescence and Application, Changchun Institute of Optics, Fine Mechanics and Physics, Chinese Academy of Sciences, Changchun 130033, China

^b Graduate School of Chinese Academy of Sciences, Beijing 100049, China

ARTICLE INFO

Article history:

Received 23 July 2013

Received in revised form 15 October 2013

Accepted 15 October 2013

Available online 26 October 2013

Keywords:

Photoluminescence

Phosphor

LEDs

ABSTRACT

A series of Eu^{3+} ions doped $\text{Sr}_9\text{Sc}(\text{PO}_4)_7$ orange–red emitting phosphors have been prepared by solid-state reaction method. Photoluminescence properties under near-ultraviolet (NUV) light excitation of the samples have been carried out. The studies show that the samples can be effectively excited by NUV (394 nm) which matches to the output wavelengths of near UV chips and exhibits intense orange–red emissions. Eu^{3+} concentration was found to be optimum at $x = 0.4$ and the thermal quenching temperature of $\text{Sr}_9\text{Sc}(\text{PO}_4)_7:0.4\text{Eu}^{3+}$ is above 200 °C. Thus, the intense orange red emitting phosphor could be a promising phosphor candidate in generating white light combined with the NUV chip.

© 2013 Elsevier B.V. All rights reserved.

1. Introduction

Phosphor-converted white light emitting diodes (LEDs) are regarded as a new lighting source for the next generation [1–3]. The present technical bottleneck is that the as-resulted white light is cool, which lacks color richness. The white LEDs demand red phosphors excited by blue or near ultraviolet (NUV) LED chips [4,5]. The commercial red phosphor $\text{Y}_2\text{O}_3:\text{Eu}^{3+}$ shows lower efficiency under NUV or blue light excitations and instability [6]. Recently, some nitrides and oxy-nitrides-based compounds have been demonstrated to be good red phosphors with high thermal stability [7–9]. However, very high firing temperatures and high nitrogen pressures are required for their synthesis, resulting in higher production cost. Therefore, it is very urgent to develop the chemically stable, environmentally friendly and high efficiency phosphors to meet the requirements for solid state lighting.

Trivalent Eu ion is considered to be one of the most important activators that emits in red color regions and many investigations have been done in many types of host materials, e.g. borates, aluminates, silicates, vanadates, phosphates, etc. [10–17]. Among them, Eu^{3+} -doped phosphates have been paid more attention due to their easy-synthesis, low-cost and chemical/thermal-stabilities over a wide range of temperatures [17–19].

In this paper, the orange–red phosphor of Eu^{3+} ions doped $\text{Sr}_9\text{Sc}(\text{PO}_4)_7$ was synthesized by a solid state reaction. The luminescence properties were investigated and discussed in detail. The results show the promising application of the as-prepared phosphor in the lighting field.

2. Experimental

The $\text{Sr}_9\text{Sc}_{1-x}(\text{PO}_4)_7$ (SSP): $x\text{Eu}^{3+}$ phosphors have been prepared by conventional solid-state reaction. The starting materials, analytical grade, SrCO_3 , Sc_2O_3 , $(\text{NH}_4)_2\text{HPO}_4$ and Eu_2O_3 were employed as the raw materials, which were mixed homogeneously by an agate mortar and pestle for 30 min, placed in a crucible with a lid, and then sintered at 1400 °C for 4 h in air.

Powder X-ray diffraction (XRD) data were collected using $\text{Cu-K}\alpha$ radiation ($\lambda = 1.54056 \text{ \AA}$) on a Bruker D8 Advance diffractometer. The photoluminescence (PL) and photoluminescence excitation (PLE) spectra were measured using a HITACHI F-7000 spectrometer. The temperature-dependent luminescence properties were measured on the same F-7000 spectrophotometer, which was combined with a self-made heating attachment.

3. Results and discussion

3.1. Crystal structure

Fig. 1 shows the XRD patterns of the SSP: $x\text{Eu}^{3+}$ samples. All of the diffraction peaks are indexed to the standard data of $\text{Sr}_9\text{Sc}(\text{PO}_4)_7$ (JPCDS card No. 54-1186) and no other phase is detected, indicating that the obtained samples are single phase and the activator ions have been successfully incorporated in the host lattices. The positions of the diffraction peaks were found to gradually move to the low degree with increasing the Eu^{3+} doping concentration x from 0.1 to 0.8, which implies that most Eu^{3+} ($R_{\text{Eu}} = 0.947 \text{ \AA}$, CN = 6) ions with large ionic radius substitute Sc^{3+} ($R_{\text{Sc}} = 0.745 \text{ \AA}$, CN = 6) ions with small ionic radius.

3.2. Photoluminescence properties of SSP: Eu^{3+}

The PLE and PL spectra of SSP:0.4 Eu^{3+} are shown in Fig. 2. The excitation spectrum detected at 590 nm consisted of a broad band

* Corresponding author. Tel./fax: +86 043186708875.

E-mail address: zhangjh@ciomp.ac.cn (J. Zhang).

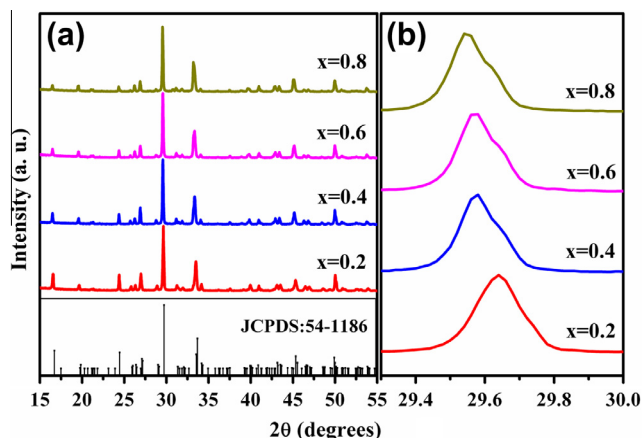


Fig. 1. (a) XRD patterns for the samples SSP: $x\text{Eu}^{3+}$ ($x = 0.1$ – 0.8). (b) Enlarged peaks in various XRD patterns.

which is attributed to the O^{2-} – Eu^{3+} charge transfer band (CTB) and a group of sharp lines in longer wavelength region. The sharp excitation peaks between 300–500 nm are assigned to the $4f \rightarrow 4f$ forbidden transitions of Eu^{3+} in the host lattice, those are correspond to the ground state ${}^7\text{F}_0$ to the excited levels ${}^5\text{F}_4$ (298 nm), ${}^5\text{H}_6$ (320 nm), ${}^5\text{D}_4$ (362 nm), ${}^5\text{L}_7$ (382 nm), ${}^5\text{L}_6$ (394 nm), ${}^5\text{D}_3$ (417 nm), ${}^5\text{D}_2$ (466 nm) transition of Eu^{3+} [20,21]. The strongest excitation line at 394 nm contributes to the ${}^7\text{F}_0$ – ${}^5\text{L}_6$ transition in the near-UV region, which matches well with the commercial near-UV LED chip.

Under the excitation of 394 nm, the phosphor SSP:0.4 Eu^{3+} exhibits intense orange-red emission. The spectrum consists of several emission lines in the region from 570 to 725 nm, originating from the transitions of the excited state ${}^5\text{D}_0$ to the ground states ${}^7\text{F}_j$ ($j = 0$ – 4). It is well known that ${}^5\text{D}_0 \rightarrow {}^7\text{F}_2$ electronic dipole transition is super sensitive to the symmetry of occupied site, while ${}^5\text{D}_0 \rightarrow {}^7\text{F}_1$ magnetic dipole transition is insensitive to that. In a site with an inversion symmetry, the magnetic dipole transition ${}^5\text{D}_0 \rightarrow {}^7\text{F}_1$ is dominant, while in a site without inversion symmetry, the ${}^5\text{D}_0 \rightarrow {}^7\text{F}_2$ electronic transition becomes the strongest one. Therefore, the $({}^5\text{D}_0 \rightarrow {}^7\text{F}_2)/({}^5\text{D}_0 \rightarrow {}^7\text{F}_1)$ intensity ratio can be used as a measure of the site symmetry of Eu^{3+} . The asymmetry ratio of $\text{Sr}_9\text{Sc}(\text{PO}_4)_7:0.4\text{Eu}^{3+}$ is 1.5. In this phosphor, the emission intensities from electric dipole ${}^5\text{D}_0 \rightarrow {}^7\text{F}_2$ transition and magnetic dipole ${}^5\text{D}_0 \rightarrow {}^7\text{F}_1$ transition have comparable intensities, indicating that more than one Eu^{3+} site in this host could be expected. However, there is only one Sc^{3+} sites in the host. That is say, part of the Eu^{3+} ions occupy Sr^{2+} sites. The detailed structure of $\text{Sr}_9\text{Sc}(\text{PO}_4)_7$ is not clear at present. The remained investigations of the structure and the site-selective luminescence should be conducted in the future experiments.

In order to obtain the best doping concentration of Eu^{3+} , a series of SSP: $x\text{Eu}^{3+}$ phosphors have been prepared. Fig. 3 presents the variation of PL intensities (integrated area from 550 to 725 nm) with different Eu^{3+} concentration. The PL intensity increases initially with the increase of Eu^{3+} concentration, and reaches the maximum at $x = 0.4$. Then, it decreases with the further increase of Eu^{3+} concentration due to the concentration quenching effect. When Eu^{3+} concentration is low, the interaction of Eu^{3+} – Eu^{3+} can be almost neglected and the emission intensity increases with the increase of Eu^{3+} concentration. With the further increase of Eu^{3+} concentration, the enhanced nonradiative energy transfer between Eu^{3+} ions will decrease the fluorescence intensity. According to Blasse, the critical distance R_c between two activator ions for most effective energy transfer in phosphors can be calculated from the critical concentration of the activator ion [22]

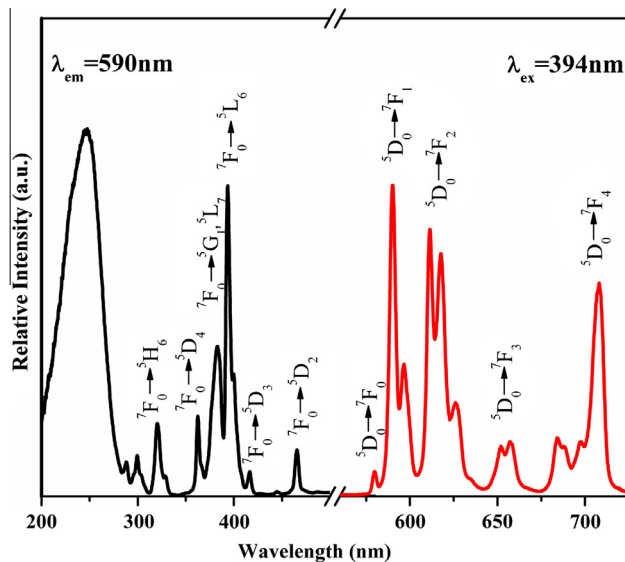


Fig. 2. PLE ($\lambda_{em} = 590$ nm) and PL ($\lambda_{ex} = 394$ nm) spectra for SSP:0.4 Eu^{3+} .

$$R_c \approx 2 \left[\frac{3V}{4\pi x_c N} \right]^{1/3} \quad (1)$$

where V is the volume of the unit cell, x_c is the critical concentration, and N is the number of lattice sites in the unit cell that can be occupied by the activator ion. For the SSP host, $N = 4$, $x_c = 0.4$, and $V = 2580.86 \text{ \AA}^3$, the obtained R_c value is 14.55 Å.

Non-radiative energy transfer between different Eu^{3+} ions may occur by radiation reabsorption, exchange interaction, or multipolar interaction. The mechanism of radiation reabsorption comes into effect only when there is a broad overlap of the emission spectrum of the sensitizer and the excitation spectrum of the activator. In the present case, Eu^{3+} ion shows the forbidden $4f \rightarrow 4f$ transition and there is no overlap between the excitation and emission spectra, the radiation reabsorption is unlikely to be occurred. The exchange interaction is generally responsible for the energy transfer of forbidden transition and the typical critical distance is about 5 Å [23]. However, the calculated R_c value of SSP: Eu^{3+} is larger than 5 Å, which implies that the exchange interaction is ineffective between Eu^{3+} in this phosphor [24]. The electric multipole interactions between Eu^{3+} ions are weak due to the weak oscillator

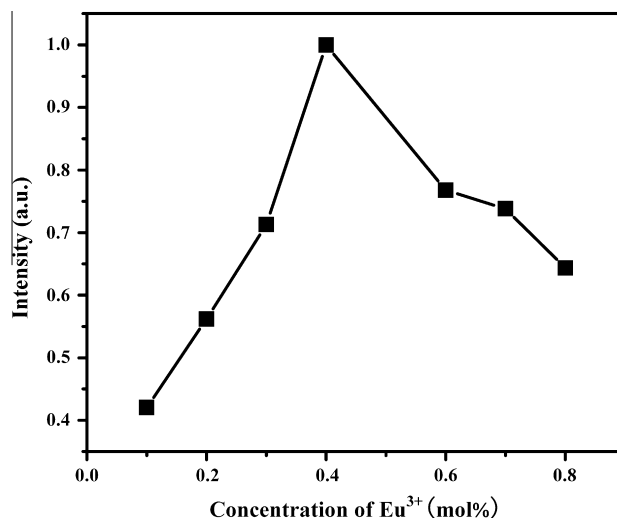


Fig. 3. Dependence of emission intensity of SSP: $x\text{Eu}^{3+}$ on the Eu^{3+} concentration.

strength of ${}^7F_0 \rightarrow {}^5D_0$ [25]. The possible mechanism of energy transfer in SSP:xEu $^{3+}$ is under investigation.

3.3. Effect of crystallographic sites of Eu $^{3+}$ on the spectra

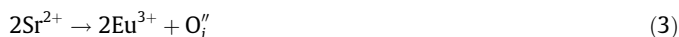
According to the PL properties in Fig. 2, it is deduced that Eu $^{3+}$ occupy Sc $^{3+}$ and Sr $^{2+}$ sites, whereas the charge compensation mechanism must be considered as Eu $^{3+}$ ions occupy the Sr $^{2+}$ sites. There are two possible ways [26]:

First, Eu $^{3+}$ ions substitute for the Sr $^{2+}$ site and combine with Sr vacancy



in which Eu $^{3+}$ ions combine with Sr $^{2+}$ vacancy to form the dipole complexes of $[2(\text{Eu}_{\text{Sr}}^{3+})^{\bullet} - V''_{\text{Sr}}]$.

The other charge compensation mechanism is related to the interstitial anion which can be expressed by the formula (3):



In this way, Eu $^{3+}$ ions form the dipole complexes of $[2(\text{Eu}_{\text{Sr}}^{3+})^{\bullet} - O_i'']$. V_{Sr}'' is an Sr vacancy with two negative charges and the O_i'' are interstitial anion. The $(\text{Eu}_{\text{Sr}}^{3+})^{\bullet}$ represents a Eu $^{3+}$ cation on a Sr $^{2+}$ site with a positive charge.

Considering the above mentioned charge compensation mechanism, the substitution of Sr $^{2+}$ sites by Eu $^{3+}$ will lead to the abnormality of crystal structure through forming the cation vacancy and interstitial anion in the hosts. The aberrance of the host micro-structure increase the probability of the optical excitation which is trapped at defects or impurity sites causing the non-radiative relaxation of Eu $^{3+}$. This is the reason for decrease in PL intensity beyond the critical concentration as shown in Fig. 3.

3.4. Thermal quenching properties

Thermal stability is an important technological parameter for pc-WLEDs. Fig. 4 shows the temperature-dependent relative emission intensities of SSP:0.4Eu $^{3+}$ phosphors measured at 23–220 °C under excitation at 394 nm. The decrease of emission intensity with increasing temperature can be attributed to the thermal quenching effect [27,28]. The thermal quenching temperature (T_{50}) is defined as the temperature at which the emission intensity is 50% of its original value [28]. When the temperature was increased to 100 °C, the relative emission intensity of SSP:0.4Eu $^{3+}$ decreased to 88%. At 200 °C, the relative emission intensity of

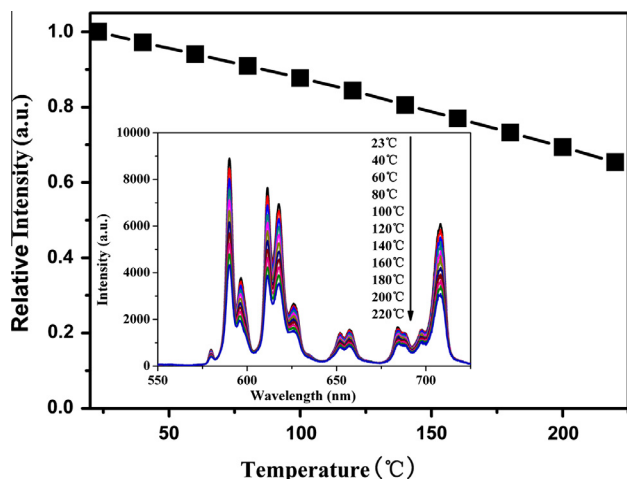


Fig. 4. Temperature dependence of the relative emission intensity for SSP:0.4Eu $^{3+}$ phosphor under 394 nm excitation.

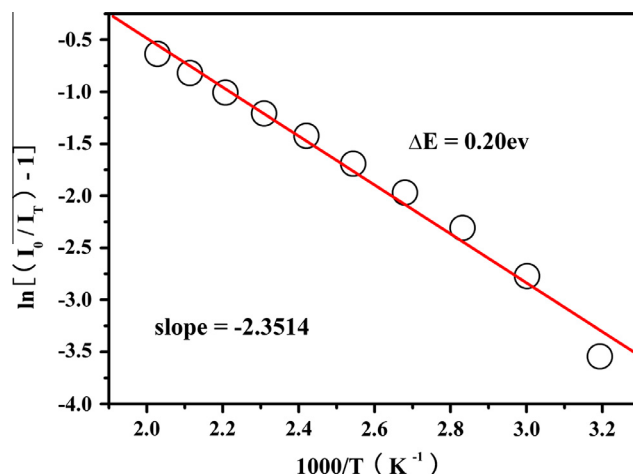


Fig. 5. The activation energy of the SSP:0.4Eu $^{3+}$ phosphor.

SSP:0.4Eu $^{3+}$ remained at 69% of that measured at 25 °C. The results show that the value of T_{50} for the phosphor is above 200 °C, indicating that this phosphor have good thermal stability. As seen in the Fig. 5, the relationship of the relative emission intensities with temperature can be used to calculate the activation energy (E_a) from thermal quenching using the following equation [29]:

$$I_T = \frac{I_0}{1 + A \exp(-\Delta E/k_B T)} \quad (4)$$

where I_0 is the initial emission intensity, I_T is the intensity at different temperatures, ΔE is activation energy of thermal quenching, A is a constant for a certain host, and k_B is the Boltzmann constant (8.617×10^{-5} eV/K). The activation energy ΔE was calculated to be 0.20 eV for the SSP:0.4Eu $^{3+}$ phosphor.

4. Conclusions

Sr $_9$ Sc(PO $_4$) $_7$:xEu $^{3+}$ phosphors were prepared through solid state reaction. Structural and optical studies of the samples were carried out. Photoluminescence studies showed that the Eu $^{3+}$ ions occupy Sc $^{3+}$ and Sr $^{2+}$ sites in SSP phosphor, thereby favoring the multiband emission. Meanwhile, the samples can be effectively excited by near UV (394 nm) light nicely matching to the output wavelengths of near UV chips and exhibits intense orange–red emissions. Eu $^{3+}$ doping concentration was found to be optimum at $x = 0.4$ and the thermal quenching temperature of SSP:0.4Eu $^{3+}$ is above 200 °C. Thus, the intense orange red emitting phosphor could be used as potential orange–red emitting phosphor candidate for n-UV based white-LEDs.

Acknowledgments

This work is supported by the National Natural Science Foundation of China (10834006, 51172226, 61275055, 11274007, 11174278) and the Natural Science Foundation of Jilin province (201205024).

References

- [1] C.C. Lin, R.S. Liu, J. Phys. Chem. Lett. 2 (2011) 1268–1277.
- [2] S. Ye, F. Xiao, Y.X. Pan, Y.Y. Ma, Q.Y. Zhang, Mater. Sci. Eng. R 71 (2010) 1–34.
- [3] C. Sommer, P. Hartmann, P. Pachler, H. Hoshopf, F.P. Wenzl, J. Alloys Comp. 520 (2012) 146–152.
- [4] T. Suehiro, R.J. Xie, N. Hiroaki, Ind. Eng. Chem. Res. 52 (2013) 7453–7456.
- [5] Q.T. Zhang, L. Zhang, P.D. Han, Y. Chen, H. Yang, L.X. Wang, Prog. Chem. 23 (2011) 1108–1122.
- [6] Z. Ju, R. Wei, X. Gao, W. Liu, C. Pang, Opt. Mater. 33 (2011) 909–913.

- [7] R.J. Xie, N. Hirotsaki, N. Kiumra, K. Sakuma, M. Mitomo, Appl. Phys. Lett. 90 (2007) 191101–191103.
- [8] J.M. Song, J.S. Park, S. Nahm, Ceram. Int. 39 (2013) 2845–2850.
- [9] Z.Y. Zhao, Z.G. Yang, Y.R. Shi, C. Wang, B.T. Liu, G. Zhu, Y.H. Wang, J. Mater. Chem. C 1 (2013) 1407–1412.
- [10] Q.Z. Dong, Y.H. Wang, Z.F. Wang, X. Yu, B.T. Liu, J. Phys. Chem. C 114 (2010) 9245–9250.
- [11] Sheetal, V.B. Taxak, Mandeep, S.P. Khatkar, J. Alloys Comp. 549 (2013) 135–140.
- [12] M.B. Xie, Y.B. Li, R.L. Li, J. Lumin. 136 (2013) 303–306.
- [13] V.B. Taxak, Sheetal, Dayawati, S.P. Khatkar, Current Appl. Phys. 13 (2013) 594–598.
- [14] E. Pavitra, G. Seeta Rama Raju, Yeong Hwan Ko, Jae Su Yu, Phys. Chem. Chem. Phys. 14 (2012) 11296–11307.
- [15] E. Pavitra, G. Seeta Rama Raju, Jin Young Park, Yeong Hwan Ko, Jae Su Yu, J. Alloys Comp. 553 (2013) 291–298.
- [16] G. Seeta Rama Raju, E. Pavitra, Jae Su Yu, Dalton Trans. 42 (2013) 11400–11410.
- [17] R.J. Yu, H.M. Noh, B.K. Moon, B.C. Choi, J.H. Jeong, K.W. Jang, S.S. Yi, J.K. Jang, J. Alloys Comp. 576 (2013) 236–241.
- [18] X.G. Zhang, L.Y. Zhou, M.L. Gong, Opt. Mater. 35 (2013) 993–997.
- [19] S. Chawla, Ravishanker, Rajkumar, A.F. Khan, R.K. Kotnala, J. Lumin. 136 (2013) 328–333.
- [20] M. Dejneka, E. Snitzer, R.E. Riman, J. Lumin. 65 (1995) 227–245.
- [21] N. Xie, Y. Huang, X. Qiao, L. Shi, H.J. Seo, Mater. Lett. 64 (2010) 1000–1002.
- [22] G. Blasse, Phys. Lett. A 28 (1968) 444–445.
- [23] G. Blasse, Prog. Solid State Chem. 18 (1988) 79–171.
- [24] Y. Wang, D. Wang, J. Electrochem. Soc. 153 (2006) H166–H169.
- [25] G. Ju, Y. Hu, L. Chen, X. Wang, Z. Mu, H. Wu, F. Kang, J. Alloys Comp. 509 (2011) 5655–5659.
- [26] F.A. Kröger, H.J. Vink, Physica 20 (1954) 950–964.
- [27] C. Ronda, Luminescence. From Theory to Applications, Wiley-VCH, Weinheim, 2008.
- [28] Y.-S. Tang, S.-F. Hu, W.-C. Ke, C.C. Lin, N.C. Bagkar, R.-S. Liu, Appl. Phys. Lett. 93 (2008) 131114. 3pp.
- [29] V. Bachmann, A. Meijerink, C. Ronda, J. Lumin. 129 (2009) 1341–1346.